

Delineation of Type I Protein Kinase A-selective Signaling Events Using an RI Anchoring Disruptor*

Received for publication, April 5, 2006, and in revised form, May 23, 2006 Published, JBC Papers in Press, May 25, 2006, DOI 10.1074/jbc.M603223200

Cathrine Rein Carlson^{‡§1,2}, Birgitte Lygren^{‡§1}, Torunn Berge[‡], Naoto Hoshi[§], Wei Wong[§], Kjetil Taskén[‡], and John D. Scott[§]

From the [‡]Biotechnology Centre of Oslo, University of Oslo, PB 1125 Blindern, N-0317, Oslo, Norway and [§]Howard Hughes Medical Institute, Vollum Institute, Oregon Health and Science University, Portland, Oregon 97239

Control of specificity in cAMP signaling is achieved by A-kinase anchoring proteins (AKAPs), which assemble cAMP effectors such as protein kinase A (PKA) into multiprotein signaling complexes in the cell. AKAPs tether the PKA holoenzymes at subcellular locations to favor the phosphorylation of selected substrates. PKA anchoring is mediated by an amphipathic helix of 14–18 residues on each AKAP that binds to the R subunit dimer of the PKA holoenzymes. Using a combination of bioinformatics and peptide array screening, we have developed a high affinity-binding peptide called RIAD (RI anchoring disruptor) with >1000-fold selectivity for type I PKA over type II PKA. Cell-soluble RIAD selectively uncouples cAMP-mediated inhibition of T cell function and inhibits progesterone synthesis at the mitochondria in steroid-producing cells. This study suggests that these processes are controlled by the type I PKA holoenzyme and that RIAD can be used as a tool to define anchored type I PKA signaling events.

The cAMP signaling pathway synchronizes a variety of physiological responses including cell proliferation and differentiation, microtubule dynamics, reproductive function, modulation of immune responses, and steroidogenesis (1–3). Many of these responses require activation of the cAMP-dependent protein kinase (PKA).³ The dormant PKA holoenzyme is a heterotetramer composed of two catalytic (C) subunits held in an inactive conformation by a regulatory (R) subunit dimer. Upon activation with cAMP, the C subunits are released from their

interaction with the R subunit dimer and are free to phosphorylate a plethora of target substrates. Individual cells express a range of PKA isozymes differing in R (RI α , RI β , RII α , RII β) and C (C α , C β , C γ) subunit composition. The type I and type II PKA isozymes, which are classified on the basis of their R subunit dimer, possess slightly different physical and biological properties including a differential sensitivity to cAMP.

Spatiotemporal regulation of PKA phosphorylation events is facilitated by A-kinase anchoring proteins (AKAPs). This family of structurally diverse but functionally related proteins act as molecular scaffolds to cluster PKA with specific substrates and signal termination enzymes such as phosphatases (4, 5) and cAMP-specific phosphodiesterases (6–9). The number of AKAPs has been estimated to more than 75, of which ~50 have been identified to date (3, 10). Although the majority of AKAPs described to date bind type II PKA via the RII regulatory subunit, several dual function AKAPs are capable of interacting with both the type I and the type II PKA holoenzyme (11–15). There are also examples of anchoring proteins such as AKAP β (16), PAP7 (17), and merlin (18) that selectively interact with the RI subunit of PKA.

The molecular basis for PKA anchoring is the interaction of an amphipathic helical motif of 14–18 residues on the AKAP with a hydrophobic groove in the N-terminal dimerization domain of the R subunit. High affinity peptides mimicking the amphipathic helix bind to the R dimer and can serve as competitive inhibitors of the PKA-AKAP interaction and inhibit signaling by delocalization of PKA. The prototypic inhibitor that has been used to disrupt PKA localization is the peptide known as Ht31 (19), which encompasses the RII binding domain of human thyroid AKAP (AKAP-Lbc) (20). Recently, the dual specificity anchoring protein D-AKAP2 has been used as a template to design peptides that preferentially interact with RI α *in vitro* (21). Here, we have conducted a bioinformatics analysis on a set of dual-affinity AKAP binding sequences to develop a peptide that binds RI α with higher affinity and specificity than any naturally occurring AKAP or other RI α -binding peptide reported. When introduced into cells, this peptide specifically disrupts anchoring of type I PKA from intracellular locations and inhibits type I PKA regulation of T cell effector function and steroid biosynthesis.

EXPERIMENTAL PROCEDURES

Autospot Peptide Array—Peptide arrays were synthesized on cellulose paper using an Autospot Robot ASP222 or a Multipex

* This work was supported by grants from The Norwegian Cancer Society, Oddrun Mjäländs Stiftelse, National Institutes of Health Grant DK54441, Heart and Stroke Foundation of Canada, The National Programme for Research in Functional Genomics in Norway (FUGE), The Research Council of Norway (MEDKAP), Birkeland Innovation AS, and European Union RTD Grant QLK3-CT-2002-02149. The costs of publication of this article were defrayed in part by the payment of page charges. This article must therefore be hereby marked "advertisement" in accordance with 18 U.S.C. Section 1734 solely to indicate this fact.

¹ These authors contributed equally.

² To whom correspondence should be addressed: Institute for Experimental Medical Research, Ullevål University Hospital, Kirkeveien 166, 0407 Oslo, Norway. Tel.: 47-23016796; Fax: 47-23016799; E-mail: cathrine.carlson@biotek.uio.no.

³ The abbreviations used are: PKA, protein kinase A; RIAD, RI anchoring disruptor; scRIAD, scrambled RIAD; AKAP, A-kinase anchoring protein; cAMP, cyclic AMP; PDSM, position-dependent scoring matrix; PKI, protein kinase inhibitor; AMPA, α -amino-3-hydroxy-5-methyl-4-isoxazolepropionic acid; ACTH, adrenocorticotrophic hormone; StAR, steroid acute response protein; LAT, linker for activation of T cells; Csk, C-terminal Src kinase; Lck, lymphocyte-specific protein-tyrosine kinase; GFP, green fluorescent protein; HEK, human embryonic kidney.

RI Anchoring Disruptor

automated peptide synthesizer (INTAVIS Bioanalytical Instruments AG) as described (22).

MEME Software—MEME software was used for consensus sequence generation (23). MEME setting included one motif per sequence, and a motif length of 24 amino acids was specified.

Helical Wheel Model Prediction and Alignments—Protean and MegAlign were used (DNASTAR Inc.).

Densitometric Analysis—The densitometric analysis was performed using Scion Image (Scion Corp.) or Quantity One Version 4.5.0 (Bio-Rad).

R-overlay—R-overlays were conducted as described using ^{32}P -labeled recombinant murine RII α (24) or bovine or human RI α (A98S) or by cold RI α -overlay. Cold RI α -overlay was performed by incubating the membrane with 250 nM RI α overnight at 4 °C and then washing the membrane five times in cold Tris-buffered saline with Tween 20 for 5 min at 4 °C. RI α was detected by immunoblotting with an RI α antibody.

Constructs and Mutagenesis—Oligonucleotides with the following sequences were cloned into the SalI and BamHI sites of pEGFP-C1, vector (Clontech): RIAD(+), 5'-GTCGACCTGGAGCAGTACGCCAACCAGCTGGCCGACCAGATCATCAAGGAGGCCACCGAGGGATCC-3'; RIAD(-), 5'-GGATCCCTCGGTGGCCTCCTTGATGATCTGGTCGGCCAGCTGGTTGGCGTACTGCTCCAGGTCGAC-3'; scRIAD(+), 5'-GTCGACATCGAGAAGGAGCTGGCCAGCAGTACCA GAACGCCGACGCCATCACCCCTGGAGGGATCC-3'; scRIAD(-), 5'-GGATCCCTCCAGGGTGATGGCGTCCGCGTTCTGGTACTGCTGGGCCAGCTCCTTCCGATGTCGAC-3' (the SalI and BamHI sites are underlined). The site-specific substitution, A98S, was made in bovine or human RI α wild type cloned into pRSET-B (Invitrogen) using a site specific-mutagenesis kit (Stratagene). Bovine RI α (Δ 1-11)(A98S), RI α (Δ 1-15)(A98S), and RI α (Δ 1-24)(A98S) mutants were made by PCR and re-cloned into pRSET-B. All constructs were confirmed by sequencing.

Fluorescence Polarization—0.5–1 nM fluorescein isothiocyanate-labeled RIAD (LEQYANQLADQIIKEATEK (5-carboxy-fluorescein)-CONH₂) and scRIAD (IEKELAQYQNADAITLEK (5-carboxyl fluorescein)-CONH₂) peptides (SynPep) were incubated with increasing concentrations of recombinant bovine RI α wt or murine RII α for 2.5 h in phosphate-buffered saline, pH 7.0, supplemented with 5 $\mu\text{g}/\mu\text{l}$ bovine serum albumin. Fluorescence polarization was measured on a Beacon 2000 fluorimeter (Panvera). Saturation binding curves were generated with PRISM graphing software (GraphPad). Dissociation constants (K_d) were calculated from the nonlinear regression curve from averages of minimum three individual experiments.

Cell Cultures—Human peripheral blood T cells were purified by negative selection as described (25). Human embryonic kidney 293 (HEK293) cells (ATCC, CRL-1573) and mouse adrenocortical Y1 cells (ATCC, CCL-79) were maintained in Dulbecco's modified Eagle's medium (DMEM) or DMEM/HAM'S F-12 respectively, supplemented with 100 $\mu\text{g}/\text{ml}$ streptomycin, 100 units/ml penicillin, and 10% (v/v) fetal calf serum in a humidified atmosphere of 5% CO₂ and split by trypsin at less than 80% confluence.

Immunoprecipitation and PKA Activity Assay—HEK293 cells at 50–80% confluency were transfected with 5–10 μg of plasmid DNA (green fluorescent protein (GFP), GFP-RIAD, GFP-scRIAD, GFP-RIAD-V5His, and GFP-scRIAD-V5His) per 56.7-cm² culture dishes using the calcium phosphate method. Cells were lysed 24 h after transfection in lysis buffer (20 mM Hepes, pH 7.5, 150 mM NaCl, 1 mM EDTA, and 1% Triton X-100) with protease inhibitors (Complete Mini EDTA-free tablets; Roche Diagnostics). Immunocomplexes were washed three times in lysis buffer before SDS/PAGE and immunoblotting. PKA kinase assays were performed by the filter paper assay (26). The protein kinase inhibitor (PKI) residues 5–24 peptide was used as a specific inhibitor of the kinase (27).

Antibodies—Immunoblotting and immunoprecipitation were carried out with antibodies against PKA RI α , RII α , and C (Santa Cruz Biotechnology or BD Transduction Laboratories), GFP (Clontech), α -tubulin (Molecular Probes), StAR (Affinity BioReagents), Lck phospho-Tyr-505 (Cell Signaling Technology), Lck (Santa Cruz Biotechnology), LAT (Linker for activation of T cells; Upstate Biotechnology Inc.), and V5 (Invitrogen). Horseradish peroxidase-conjugated anti-mouse or anti-rabbit IgGs was used as a secondary antibody (Jackson ImmunoResearch Laboratories Inc.). For immunofluorescence, antibodies against RI α (Biogenesis Ltd.), RII α (BD Transduction Laboratories), and AKAP450 (A24 (9)) plus Alexa-488- or Alexa-555-conjugated anti-mouse and anti-rabbit IgG (Molecular Probes) were used.

Immunofluorescence—Immunofluorescence was performed on T cells or Y1 adrenocortical cells attached to poly-lysine or collagen/fibronectin-coated coverslips. Mitochondria were stained with MitoTracker Red CMXRos (Molecular Probes), which was diluted in fresh medium and incubated on cells at 37 °C for 30 min before cell fixation. All cells were washed in phosphate-buffered saline, fixed with 3% paraformaldehyde, and permeabilized using 0.1% Triton X-100. Proteins were blocked in 2% bovine serum albumin/phosphate-buffered saline with Tween-20 before antibody labeling. Primary and secondary antibodies were used at a 1:200 dilution in bovine serum albumin/phosphate-buffered saline with Tween-20 and incubated for 30 min. DNA was counterstained using TO-PRO3 (Molecular Probes) at a concentration of 1 μM . Cells were examined using a Leica TCS SP1 confocal fluorescence microscope (63 \times magnification) (Leica, Germany).

Protein Expression and Purification—Bovine RI α or murine RII α was expressed in *Escherichia coli* BL21 by isopropyl 1-thio- β -D-galactopyranoside induction and purified with cAMP beads (Sigma-Aldrich) as previously described (28). Murine RII α was purified by the His tag using fast protein liquid chromatography.

Peptide Synthesis and Loading—RIAD and scRIAD (scrambled RIAD) were synthesized untagged or with 11 arginine residues at the C termini and purified to >80% purity (SynPep or in house). The arginine-coupled peptides were added directly to the cell culture (0–30 μM) at different time intervals. The peptide concentrations used were re-calculated after exact determination by Applied Biosystems Analyzer 421 (Applied Biosystems).

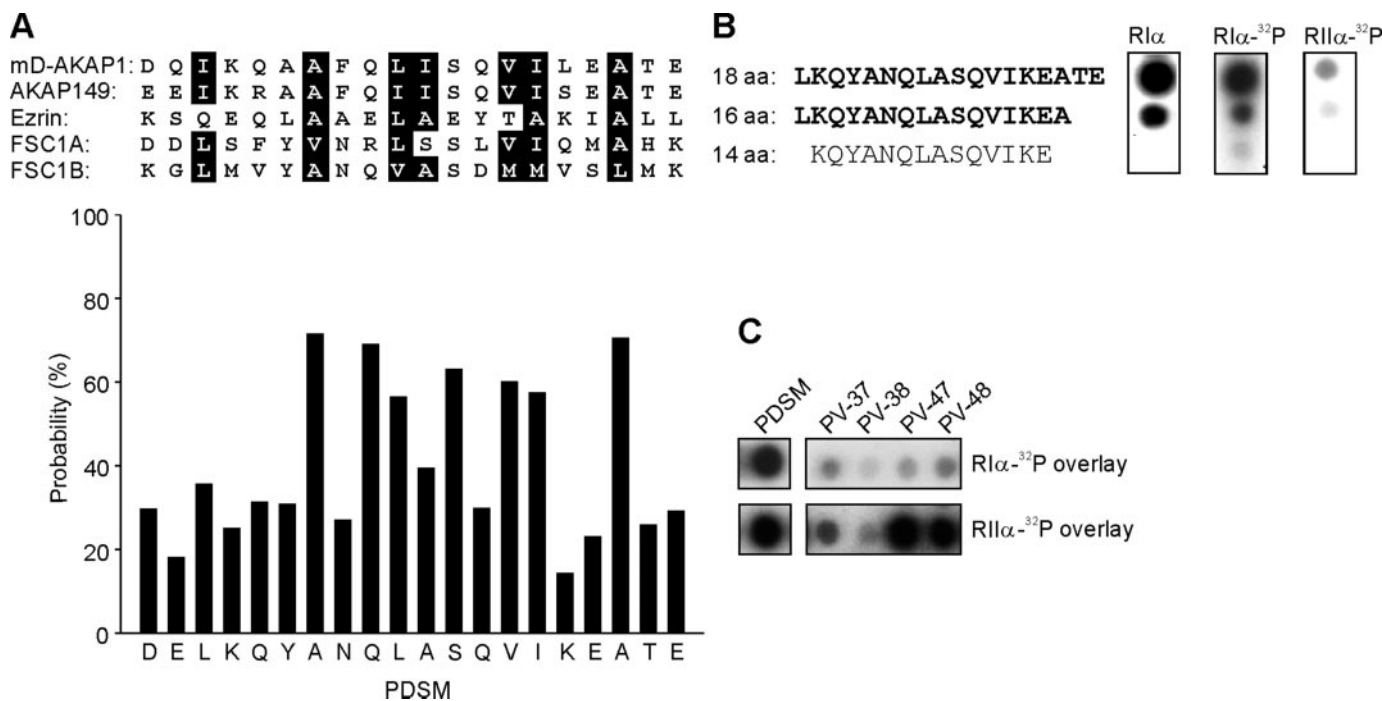


FIGURE 1. Development of an RI α binding consensus sequence. *A*, amphipathic helical motifs from mouse D-AKAP1, human AKAP149, human ezrin, and human AKAP82 (two motifs, FSC1A and FSC1B) were aligned to make an RI α binding consensus sequence. Hydrophobic amino acids matching the consensus sequence are in *black* (upper panel). Using the MEME algorithm, a PDSM was calculated representing the probability of an amino acid at a given position divided by the frequency that this amino acid is found in the nonredundant protein data base (lower panel). *B*, the minimal RI α binding sequence was determined by truncating the peptide from both the N and C termini. Binding of RI α and RII α was detected by autoradiography ($[^{32}\text{P}]\text{RI}\alpha$ (A985) and $[^{32}\text{P}]\text{RII}\alpha$ overlay) and immunoblotting using a monoclonal antibody against wild type RI α . *C*, R binding was analyzed by $[^{32}\text{P}]\text{RI}\alpha$ and $[^{32}\text{P}]\text{RII}\alpha$ overlays of the RI α binding consensus sequence versus a previously characterized RI α -selective anchoring sequence, PV-38 (21).

Circular Dichroism—CD spectra were recorded using a Jasco J-810 spectropolarimeter (Jasco International Co., Ltd., Japan) as described (29).

Progesterone Production—Y1 adrenocortical cells were cultured overnight in 6-well plates at a density of 1.5×10^6 cells per well. To increase the basal level of StAR, the cells were pre-stimulated with 10 μM forskolin for 1 h before peptide loading. The cells were loaded with the arginine-coupled peptide for 5 h, then treated with 5 $\mu\text{g}/\text{ml}$ actinomycin D (Sigma) for 30 min and finally stimulated with 10 μM forskolin (Calbiochem) or 10 IU/ml ACTH (Sigma) for 12 h. Media from cultures were collected, and progesterone levels were measured by radioimmunoassay (Spectra, Orion Diagnostica) or fluorometric assay (Delfia, PerkinElmer Life Sciences) following the manufacturers' instructions.

Solid Phase Assay—Lysates prepared from 5×10^6 Y1 adrenocortical cells were incubated at 4 $^\circ\text{C}$ overnight with RIAD and scRIAD peptides synthesized on membranes. The membranes were washed twice for 10 min in lysis buffer (150 mM NaCl, 1% Nonidet P-40, 0.5% deoxycholate, 0.1% SDS, and 50 mM Tris-HCl, pH 7.8) and thereafter in high salt lysis buffer containing 1 M NaCl before boiling in SDS-PAGE loading buffer.

Lipid Raft Purification—Isolation of lipid rafts was performed as described (30).

Electrophysiology—Whole-cell recordings were made with an Axopatch200B amplifier (Axon Instruments, Foster City, CA). Patch pipettes (2–4 megaohms) contained 140 mM cesium methanesulfonate, 5 mM adenosine triphosphate, 5 mM MgCl_2 , 0.2 mM CaCl_2 , 1 mM BAPTA (1,2-bis(2-aminophe-

noxy)ethane-*N,N,N',N'*-tetraacetate) and 10 mM HEPES, pH 7.4. Extracellular solution contained 150 mM NaCl, 5 mM KCl, 1.8 mM CaCl_2 , 10 mM glucose, 0.1 mM cyclothiazide, and 10 mM HEPES, pH 7.4. Solution exchanges were accomplished through a two-barrel pipe controlled by a solution stimulus delivery device, SF-77B (Warner Instruments, Hamden, CT). The GluR1 (AMPA channel subunit) receptor currents were evoked by a 500-ms application of 1 mM glutamate at 30-s intervals. Data were acquired and analyzed by using PCLAMP software (Axon Instruments). Currents were digitized at 5 kHz and filtered at 1 kHz.

Statistics—One-way analysis of variance with Tukey's post test was performed using GraphPad InStat version 3.00 (GraphPad).

RESULTS

Development of an Optimal RI α Binding Consensus Sequence—In an attempt to define an optimal and specific peptide disruptor for type I PKA, we used the MEME algorithm to analyze the R binding domains from several anchoring proteins that interact with RI α (23). This program looks for sites of amino acid similarity and predicts the side chain most likely to occupy a particular site on the basis of comparison to corresponding sites in the sample proteins in a nonredundant data base. The linear R binding sequences from D-AKAP1 (11), AKAP149 (31), ezrin,⁴ and AKAP82 (two sites: FSC1A and FSC1B) (13, 14) were aligned (Fig. 1A, upper panel) and analyzed by this approach. A position-de-

⁴ A. Ruppelt, M. Grönholm, E. M. Aandahl, D. Tobin, C. R. Carlson, H. Abrahamson, F. W. Herberg, O. Carpen, and K. Taskén, submitted for publication.

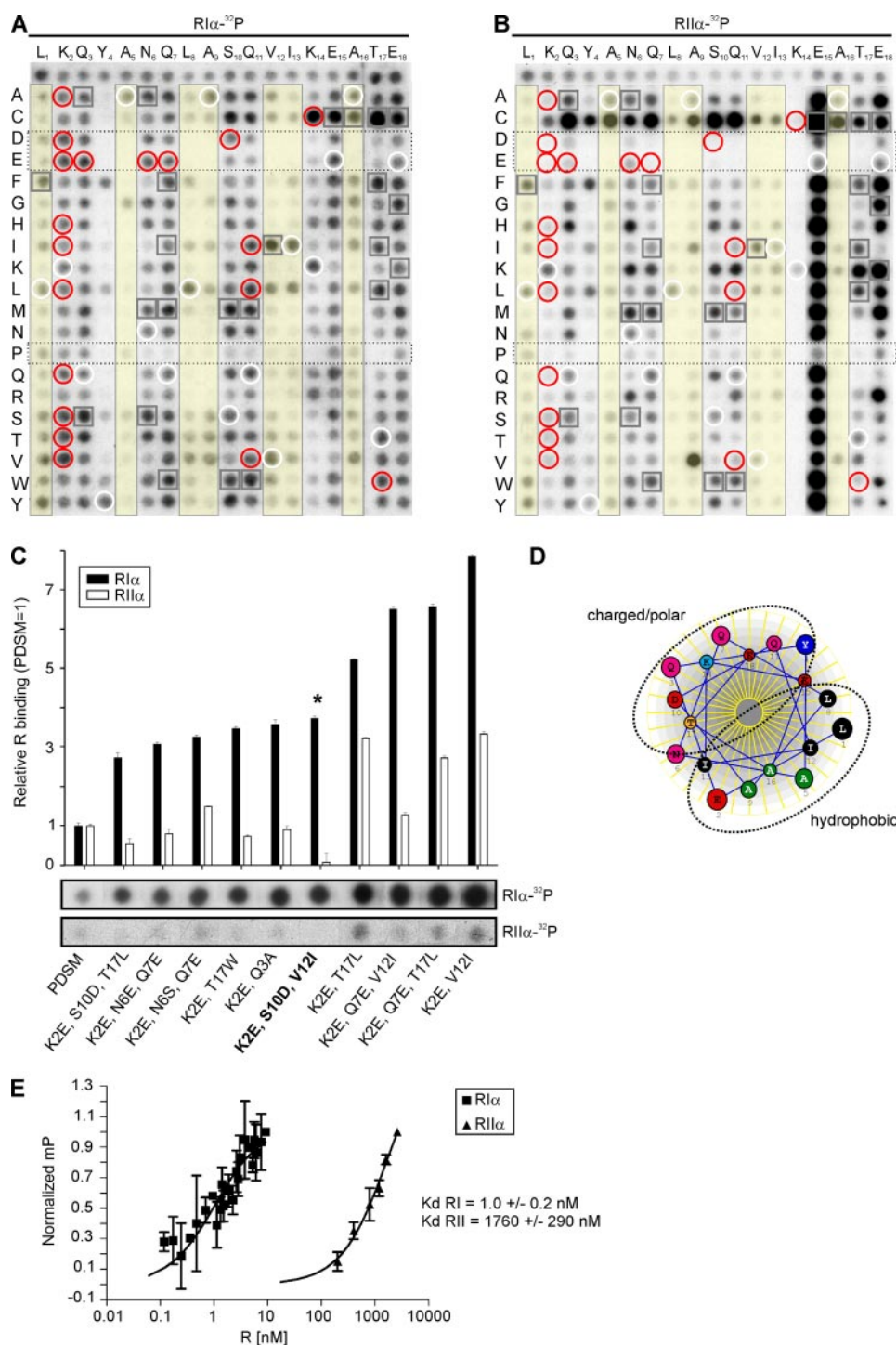


FIGURE 2. Optimization of the RI α binding consensus sequence. Two-dimensional arrays of 360 PDSM peptide derivatives are shown where each residue in the native peptide (given by their *single-letter codes* above each array) was systematically substituted with every possible residue (given by their *single-letter codes* to the left of each array). The first row in each array corresponds to the native peptide. R binding was analyzed by either [³²P]RI α (A) or [³²P]RII α (B) overlay and autoradiography. Peptide derivatives with substitutions at positions 1, 5, 8, 9, 12, 13, and 16 (yellow columns), aspartic acid, glutamic acid, and proline substitutions (dotted rectangle) and internal control peptides of native sequence (white circle) are indicated. The single substitutions K2A, K2D, K2E, K2H, K2I, K2L, K2Q, K2S, K2T, K2V, Q3E, N6E, Q7E, S10D, Q11I, Q11L, Q11V, K14C, or T17W increased the RI α binding relative to RII α binding (red circles), whereas L1F, Q3A, Q3S, N6A, N6M, N6S, Q7F, Q7I, Q7M, Q7W, S10M, S10W, Q11M, Q11W, V12I, E15C, A16C, T17C, T17F, T17I, T17L, E18C, E18G, or E18K generally increased binding to either R subunit (gray squares) ($n = 3$). C, relative R binding of ten derivatives versus the PDSM sequence and quantification by densitometry of the autoradiograms (means \pm S.E. from $n = 3$). D, α -helical wheel representation of RIAD. E, in solution binding of RIAD to RI α and RII α . Saturation binding curves were generated with increasing concentrations of R protein. Polarization values (mP) were determined at equilibrium and normalized to the highest value of saturation (means \pm S.E., $n = 3$). Non-linear regression analysis was used to derive K_d values. No interaction was detected with scRIAD.

pendent scoring matrix (PDSM) consensus sequence of 20 amino acids was identified (Fig. 1A, lower panel).

Further characterization of this sequence was performed using peptide arrays (Figs. 1, B and C). Direct binding of RI α to the immobilized peptides was made possible using RI α (A98S), a mutant R subunit form that can be phosphorylated by the C subunit of PKA *in vitro* (32). Detection of phosphorylated RI α (A98S) binding with the PDSM sequence and other immobilized AKAP-derived peptides was assessed by autoradiography (Fig. 1B). A series of peptide truncations from both the N and C termini was screened to narrow down the RI α binding site to an 18-amino acid peptide (Fig. 1B). This 18-residue PDSM sequence bound RI α (A98S) more tightly than the native AKAP peptide sequences (data not shown). Although we were able to generate an RI α selective binding peptide, the 18-residue PDSM sequence retained the ability to bind RII α as assessed by the solid phase binding assay (Fig. 1C).

Optimization of the RI α Binding Consensus Sequence and Development of RIAD—Optimization of the 18-residue PDSM sequence to enhance its preference for RI was performed by screening a two-dimensional peptide array using radiolabeled RI α as a probe (Fig. 2). 360 PDSM sequence peptide derivatives were arrayed with single side chain substitutions at each position. [³²P]RI α and -RII α binding were assessed by autoradiography (Figs. 2, A and B). The binding of each modified peptide was compared with that of internal control peptides of the original sequence (white circles). As with previous studies, we discovered that introduction of helix-breaking side-chains or removal of hydrophobic side-chains diminished RI α and RII α binding. However, introduction of acidic amino acids (aspartic acid (D) or glutamic acid (E)) at strategic positions within the sequence retained RI α binding and yielded peptides that bound poorly to RII α (dotted columns in Figs. 2A and 2B).

Nineteen single amino acid substitutions increased the relative RI α binding of the PDSM sequence over RII α (red circles in Figs. 2, A and B). This finding was exploited in a second round of peptide arrays where single-, double-, and triple-substituted peptides were screened for preferential interaction with RI α (Fig. 2C). Densitometry of autoradiographs was used to quantify the relative RI α and RII α binding of each peptide. We were able to identify a triple-substituted peptide LEQYANQLADQIIKEATE that retained a high affinity for RI α but did not appreciably bind to RII α (Fig. 2C). This peptide exhibited a 3.7-fold increase in RI α binding affinity over the original PDSM

and exhibited an apparent 50-fold selectivity for RI α over RII α . We named this RI α -binding peptide RI anchoring disruptor (abbreviated as RIAD).

Characterization of RIAD in Vitro—The helicity of RIAD and scRIAD measured by circular dichroism (CD) was 9 and 16% in water, respectively. In the presence of 50% trifluoroethanol, which induces and stabilizes α -helical structures, RIAD and scRIAD yielded CD spectra typical for α -helical peptides (data not shown), with calculated helical contents of 79 and 61%, respectively. RIAD fused to 11 arginine residues (RIAD-Arg₁₁), which was used in functional studies described below, displayed a helicity of 65% in 50% trifluoroethanol (data not shown). Modeling the RIAD sequence on a helical wheel (DNA-STAR) suggested that it consists of one clearly defined hydrophobic face and a negatively charged polar face (Fig. 2D). When this model is reconciled with our two-dimensional peptide array analysis, it suggests that changes in the hydrophobic face are not well tolerated for R subunit interaction, whereas amino acid substitutions in “non-contacting face” are important to enhance high affinity interaction with RI α .

RIAD and a control peptide with a scrambled sequence (scRIAD: IEKELAQYQNADAITLE) were synthesized with fluorescein isothiocyanate and used in fluorescence polarization assays to measure the dissociation constants of RIAD for both R subunits. Dissociation constant (K_d) for RIAD interaction with RI α was calculated to be 1.0 ± 0.2 nM ($n = 3$) (Fig. 2E). In contrast, RII α bound poorly to RIAD with a dissociation constant of 1760 ± 290 nM ($n = 3$) (Fig. 2E). Control experiments showed that the scRIAD peptide exhibited no affinity for RI or RII (data not shown). Thus, RIAD exhibits a 1760-fold preference for RI α over RII α . This suggests that RIAD is 20-fold more selective for RI α than PV-38, a peptide derived from the dual specificity anchoring protein D-AKAP1 (21). RIAD bound with similar affinity to human and bovine RI α as assessed by the solid phase overlay assay (data not shown).

Cellular Characterization of RIAD—A variety of approaches was used to characterize the interaction of RIAD with the type

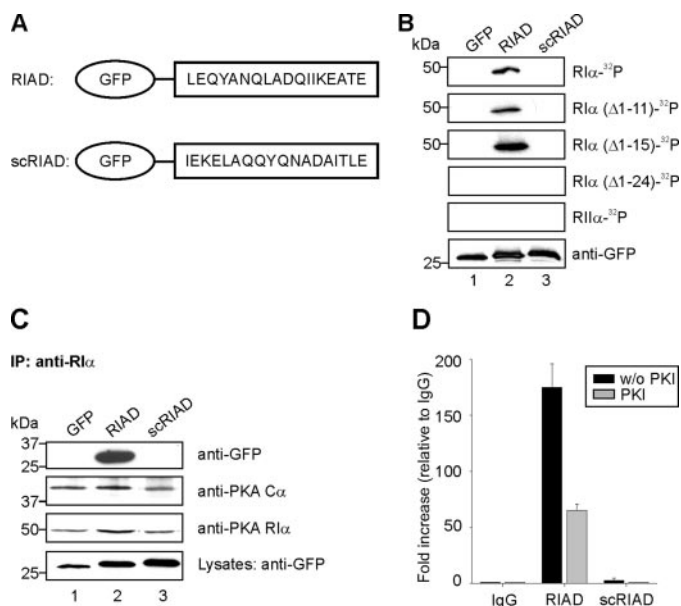


FIGURE 3. Interaction of RIAD with RI α in situ. A, schematic representation of the chimeric GFP-RIAD and GFP-scRIAD proteins used. B, lysates from HEK293 cells transfected with GFP-RIAD or GFP-scRIAD constructs were analyzed for R binding by [32 P]RI α or [32 P]RII α overlay. The levels of chimeric proteins in the lysates were analyzed by anti-GFP. C, coprecipitation of chimeric GFP-RIAD and RI α as well as levels of GFP in the lysates were detected by immunoblotting with anti-GFP. D, PKA kinase activity in GFP-RIAD immune complexes. IgG and GFP-scRIAD precipitates were used as negative controls. IP, immunoprecipitation; w/o, without.

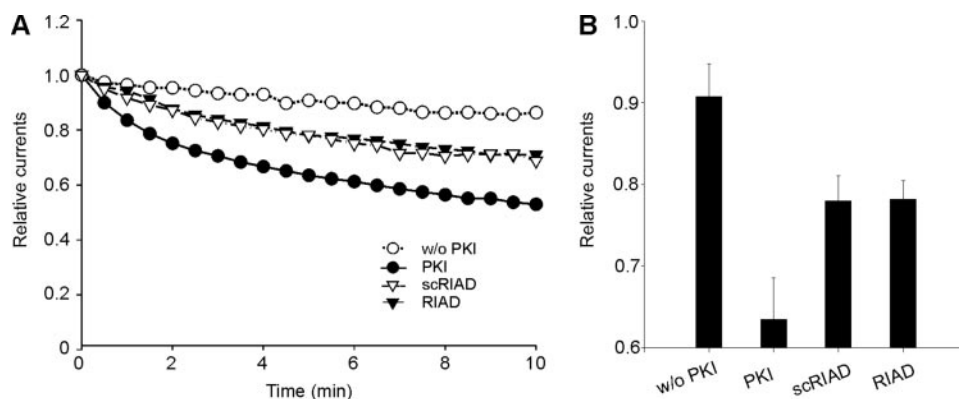
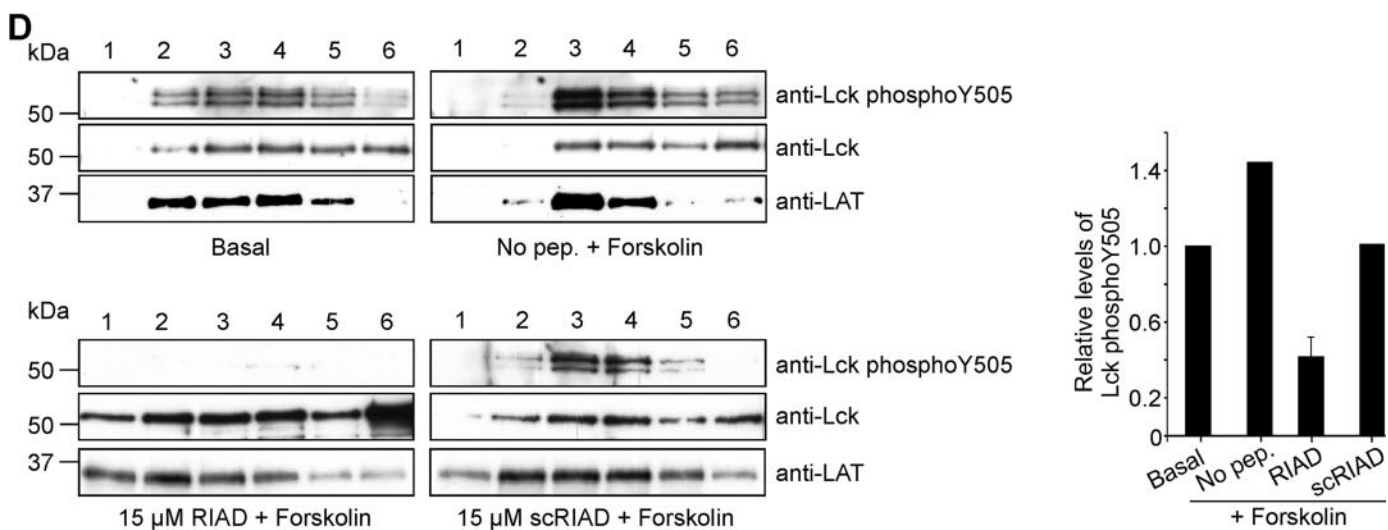
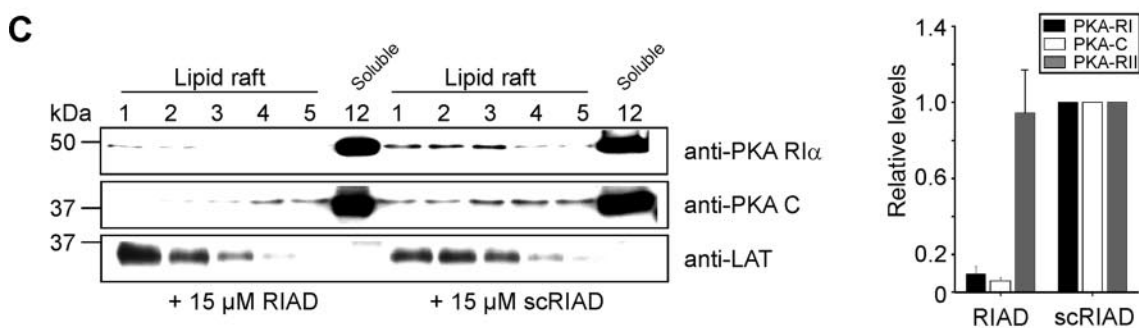
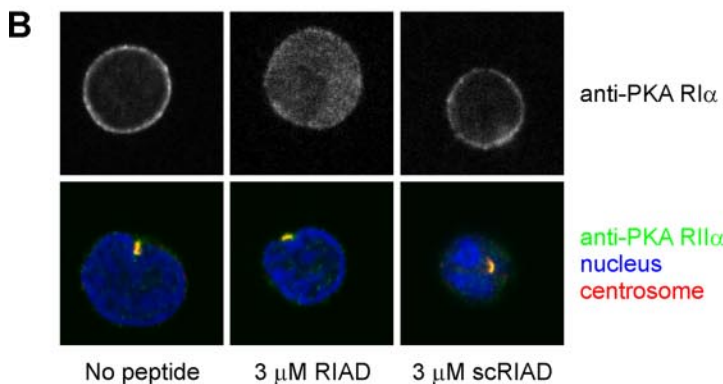
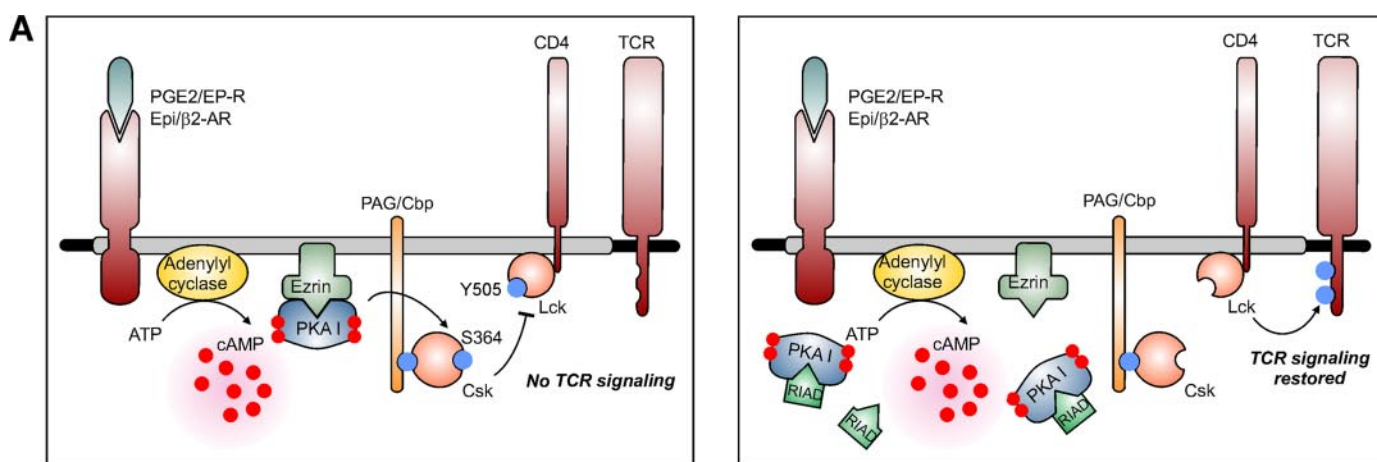


FIGURE 4. The effect of RIAD on the type II PKA signaling pathway in hippocampal neurons. A, the effect of RIAD on time-dependent rundown of AMPA-responsive currents in hippocampal neurons was analyzed by using whole-cell patch clamp recording technique. PKI (PKA inhibitor) was used as a positive control, and the scrambled control peptide, scRIAD, was used as a negative control. Representative current traces from 0 to 10 min are shown. B, graphical representation of the peak current amplitudes upon glutamate stimulation 5 min after delivery of the peptides (indicated below each column). Each bar is normalized to the peak amplitude found at time 0. PKI was used at $10 \mu\text{M}$, and other peptides were used at a concentration of $1 \mu\text{M}$ (means \pm S.E. from $n = 3$).

I PKA in HEK293 cells. Chimeric constructs encoding RIAD or scRIAD fused to the GFP were transfected into HEK293 cells (Fig. 3A). Lysates from transfected cells were prepared, subjected to SDS-PAGE, and used for an RI α overlay assay. The chimeric RIAD bound with high affinity to RI α (Fig. 3B, lane 2). Interestingly, the N-terminal-truncated RI α ($\Delta 1-15$) bound RIAD with a higher affinity, suggesting that the RI α mutant has a more accessible AKAP binding surface. Control experiments confirmed that [32 P]RI α did not bind to scRIAD-GFP chimeric protein (negative control) (Fig. 3B, lane 3).

To determine whether endogenous PKA binds to RIAD, co-immu-

RI Anchoring Disruptor



noprecipitations with an RI α antibody were performed from transfected HEK293 cells. GFP-RIAD co-purified with endogenous RI α (Fig. 3C, lane 2), whereas GFP-scRIAD did not (Fig. 3C, lanes 3). Control immunoprecipitation experiments using an RII antibody were negative (data not shown). Roughly equivalent amounts of fusion proteins were present in the immune complexes as assessed by immunoblotting with anti-GFP (lower panel). In reciprocal experiments, PKA activity co-immunoprecipitated with GFP-RIAD but not with GFP-scRIAD, as measured in an *in vitro* kinase assay using Kemptide as substrate (Fig. 3D). PKA activity was 170-fold higher in the GFP-RIAD fraction than in the fraction with only IgG. Kinase activity did not co-purify with the GFP-scRIAD, which is unable to bind PKA. Control experiments confirmed that most of the kinase activity was blocked by the PKI (5–24) peptide, a specific inhibitor of PKA (Fig. 3D, gray bars). Collectively, the experiments in Fig. 3 suggest that RIAD interacts with type I PKA isozyme inside cells.

RIAD Does Not Attenuate Type II PKA-selective Phenomena; the Rundown of Hippocampal AMPA-responsive Currents—Our biochemical studies suggest that RIAD is a selective reagent that disrupts type I PKA anchoring inside cells. To test this hypothesis, we determined whether application of RIAD had any effect on signaling events thought to be mediated by type II PKA anchoring. A physiologically relevant model is the time-dependent down-regulation (rundown) of α -amino-3-hydroxy-5-methyl-4-isoxazolepropionic acid (AMPA)-responsive currents in hippocampal neurons after the addition of glutamate, which requires an anchored pool of type II PKA as demonstrated by anchoring disruption using the Ht31 anchoring disruption peptide (33). Whole-cell patch clamp techniques provided a sensitive means to record the current upon delivery of the different bioactive peptides through the patch pipette. A control experiment confirmed that perfusion of PKI peptide (PKA inhibitor) or an RII specific peptide⁵ resulted in a rapid reduction in the current (Figs. 4, A and B). In contrast, perfusion of RIAD did not affect the AMPA-responsive currents; neither did the negative control scRIAD. Thus, RIAD does not appear to perturb a PKA type II signaling pathway.

Restoration of cAMP-inhibited T Cell Receptor Signaling by RIAD-Arg₁₁—Having established that RIAD was unable to block cellular functions attributed to type II PKA, it was important to establish whether this peptide could uncouple anchored signaling events that are mediated by type I PKA. T cell function is inhibited by cAMP (34–36), which occurs through a mechanism that involves type I PKA phosphorylation and activation of the C-terminal Src kinase (Csk) (37–40). Activated Csk in turn phosphorylates a tyrosine residue in the C terminus of Lck

505 (Tyr-505), which inhibits Lck and consequently leads to disruption of T cell signaling to the nucleus (Fig. 5A, left panel) (41). Because cAMP-mediated inhibition of T cell function is thought to require anchoring of type I PKA to the RI selective AKAP, ezrin,⁴ we wanted to test whether disruption of PKA anchoring by RIAD perturbed these events. Cell-permeable RIAD and scRIAD derivatives were generated by coupling 11 arginine (Arg₁₁) residues to the C termini of the peptides (RIAD-Arg₁₁ and scRIAD-Arg₁₁). Application of RIAD-Arg₁₁ displaced and delocalized PKA-RI α from the cell membrane of T cells as demonstrated by immunofluorescence (Fig. 5B, upper panel), whereas no displacement of PKA-RII α from the Golgi-centrosomal area (42) was observed (Fig. 5B, lower panel). Control experiments confirmed that scRIAD-Arg₁₁ peptide had no effect on PKA localization in these cells.

Lipid raft fractions isolated from T cells by sucrose gradient centrifugation were assessed for levels of PKA. In cells treated with RIAD-Arg₁₁, levels of lipid raft-associated PKA-RI α were reduced by 80–90% (Fig. 5C, left panel, and bar graph in right panel). Similarly, levels of PKA-C were reduced, whereas levels of PKA-RII α were unchanged (right panel). LAT, an adaptor protein constitutively expressed in lipid rafts (43, 44), was used as an internal standard.

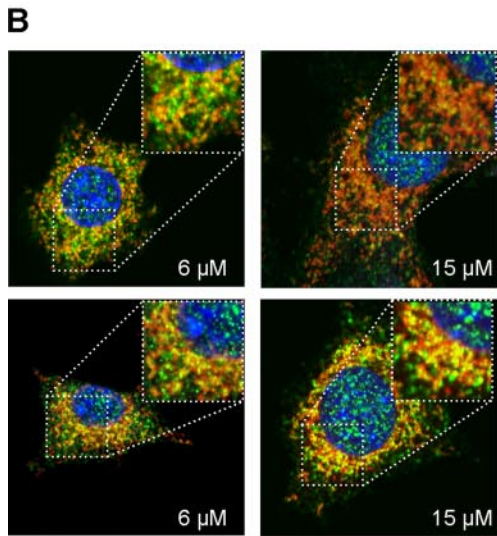
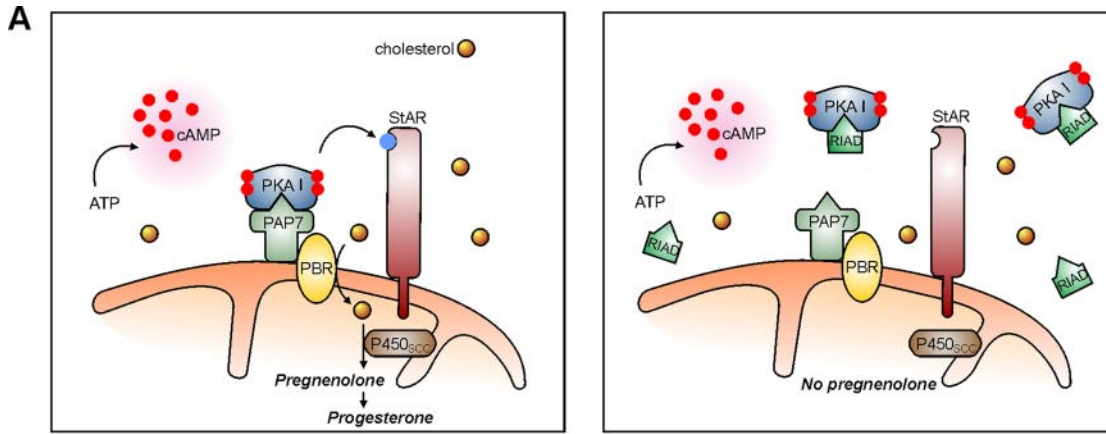
To assess the effect of RIAD on cAMP regulation of T cell function, the phosphorylation status of Tyr-505 in Lck was analyzed. When cells were treated with forskolin to activate the PKA-Csk inhibitory pathway, a 50% increase in the level of Lck Tyr-505 phosphorylation was observed in lipid raft fractions (Fig. 5D, upper right versus upper left panel and bar graph). In contrast, Lck Tyr-505 phosphorylation levels were decreased rather than increased when the cells were pretreated with 15 μ M RIAD-Arg₁₁ (lower left panel) compared with cells treated with scRIAD-Arg₁₁ (lower right panel) or untreated cells (upper left panel). In conclusion, displacement of type I PKA from lipid rafts by RIAD perturbs the cAMP-PKA-Csk inhibitory pathway in T cells. Thus, the negative regulation of T cell function by type I PKA signaling can be blocked by RIAD (Fig. 5A, right panel).

Inhibition of Hormone-stimulated Steroid Biosynthesis by RIAD-Arg₁₁—The first step in steroid biosynthesis is the conversion of cholesterol to pregnenolone by the p450 side chain cleavage enzyme (p450_{sc}) (45, 46). The enzyme is localized in the inner mitochondrial membrane and requires the transport of cholesterol from lipid droplets across the outer mitochondrial membrane by the peripheral benzodiazepine receptor (PBR) (Fig. 6A, left panel). This process is facilitated by the steroid acute response protein (StAR), which is a PKA substrate. StAR phosphorylation is a marker for acute hormonal regulation of steroid biosynthesis by adrenocorticotrophic hormone (ACTH) or luteinizing hormone in adrenocortical cells and ovarian theca cells, respectively (47, 48). Type I PKA

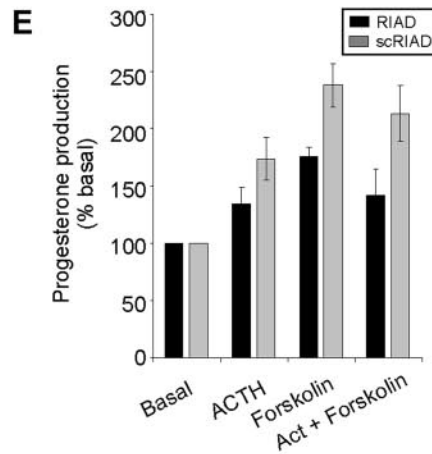
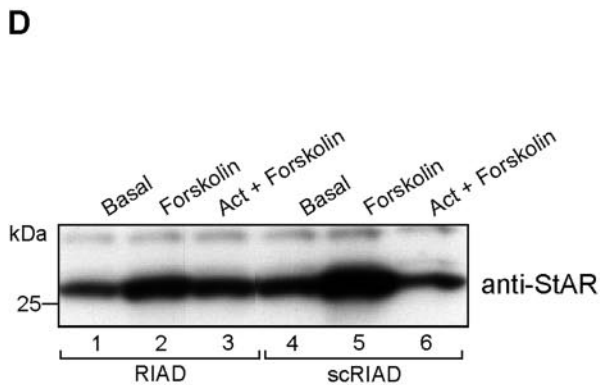
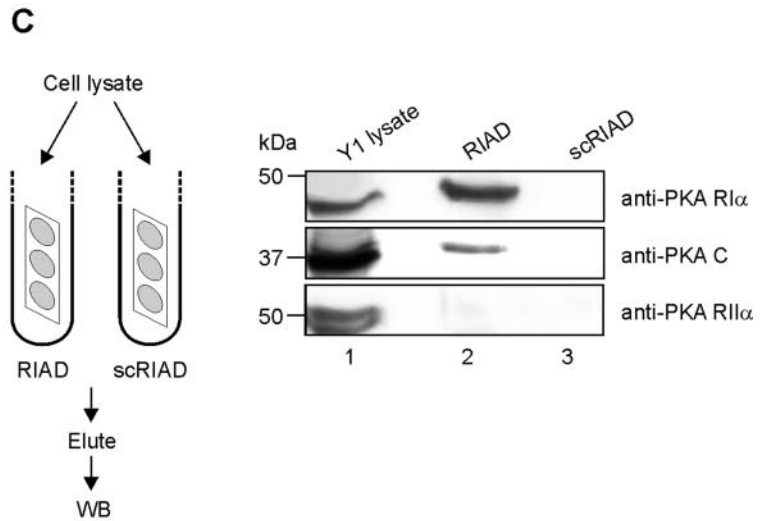
⁵ M. G. Gold, B. Lygren, P. Dokurno, N. Hoshi, G. McConnachie, K. Taskén, C. R. Carlson, J. D. Scott, and D. Barford, submitted for publication.

FIGURE 5. Effect of RIAD-Arg₁₁ on cAMP-inhibited T cell receptor signaling. A, the anchored PKA-Csk signaling pathway down-regulates T cell function (left panel), whereas anchoring disruption reverses this inhibition (right panel). PGE, prostaglandin E; TCR, T cell receptor. EP-R, E prostanoid receptor; β 2-AR, β 2-adrenergic receptor; PAG, protein associated with glycosphingolipid-enriched microdomains. B, the subcellular localization of PKA-RI α (upper panel) and PKA-RII α (lower panel) in cells treated with RIAD-Arg₁₁, was analyzed by immunofluorescence. scRIAD-Arg₁₁-treated and untreated cells were used as negative controls. C, the relative levels of PKA-RI α , PKA-C, and PKA-RII α in lipid rafts isolated from cells treated with 15 μ M RIAD-Arg₁₁ or 15 μ M scRIAD-Arg₁₁ were assessed by immunoblotting (left panel) and measured by densitometry of the autoradiograms (right panel, means \pm S.E. from $n = 4$). LAT was used as a marker for lipid raft fractions and used as an internal standard. D, levels of Lck Tyr-505 phosphorylation in basal and forskolin-stimulated cells treated with 15 μ M RIAD-Arg₁₁ or 15 μ M scRIAD-Arg₁₁ were assessed by immunoblotting with antibodies against Lck phospho-Tyr-505 (left panels) and measured by densitometry (right panel, means \pm S.E. from $n = 3$). No pep, no peptide.

RI Anchoring Disruptor



anti-PKA RI
mitochondria
nucleus



anchoring to the mitochondria via its interaction with PAP7 is thought to be necessary for this regulation (17). To test this hypothesis we applied RIAD-Arg₁₁ or scRIAD-Arg₁₁ to Y1 adrenocortical cells. In cells treated with 15 μM RIAD-Arg₁₁, endogenous RI α was displaced from mitochondria, as indicated by the lack of co-localization between RI α immunofluorescence (green) and Mitotracker, a mitochondria-specific marker (red; Fig. 6B, upper panel). In contrast, in cells treated with scRIAD-Arg₁₁, RI α localized to mitochondria, as assessed by the overlap of the RI α immunofluorescent signal with Mitotracker (yellow; Fig. 6B, lower panel).

Biochemical approaches were also used to examine the selective interaction of RIAD with the type I PKA in Y1 adrenocortical cell lysates (Fig. 6C). Cell lysates were incubated with filters containing immobilized RIAD or scRIAD peptides. The filters were extensively washed, and co-purifying proteins were eluted from the solid phase support (Fig. 6C, schematic). Immunoblot analysis of the eluates demonstrated that RIAD was able to co-purify RI α and the C subunit of PKA but not RII α (Fig. 6C, right panel, lane 2). None of the PKA subunits co-purified with the scRIAD peptide control (Fig. 6C, right panel, lane 3). Thus, RIAD selectively interacts with type I PKA holoenzyme in Y1 adrenocortical cells and can be used to selectively disrupt the location of this kinase subtype in these cells.

To assess the importance of type I PKA-dependent anchoring on phosphorylation of StAR and on steroid biosynthesis, we first looked at the StAR protein levels since they affect cholesterol transport capacity. StAR levels were up-regulated by cAMP (Fig. 6D, lanes 4 and 5), and interestingly, this up-regulation was reduced in RIAD-Arg₁₁-treated cells (Fig. 6D, lane 2). To isolate the effect of RIAD-Arg₁₁ on PKA phosphorylation of StAR, actinomycin D was used to block protein synthesis and clamp StAR levels (Fig. 6D, lanes 3 and 6). Progesterone levels increased 1.7–2.5-fold upon stimulation of Y1 adrenocortical cells with ACTH or forskolin in the presence of the control peptide scRIAD-Arg₁₁ (Fig. 6E). In cells where StAR levels had been clamped by actinomycin D, the progesterone levels were induced 2-fold in the presence of control peptide. In the presence of RIAD-Arg₁₁, progesterone production was reduced compared with control-treated cells stimulated with ACTH or forskolin ($p < 0.001$) or forskolin-stimulated cells clamped with actinomycin D ($p < 0.01$) (Fig. 6E). In the latter experiment where the effect of StAR phosphorylation was isolated, RIAD-Arg₁₁ treatment reduced progesterone production almost back to basal levels, and the inhibition was $\sim 80\%$ that observed when

the PKA phosphorylation site in StAR was mutated (49). When taken together, our results show that type I PKA-dependent anchoring is required for hormonal regulation of steroid production at the level of StAR phosphorylation.

DISCUSSION

Here, we report the development of the RI α -specific anchoring peptide, RIAD, an 18-amino acid peptide that displays a 3 orders of magnitude selectivity of binding to type I PKA over type II PKA. RIAD binds type I with a higher affinity than any natural AKAP or other anchoring disruption peptides published so far. The affinity of RIAD for RI α is 5 times greater than PV-38 (21) and 20 times more RI α -specific. Compared with Ht31, RIAD has a 1300 times higher RI α affinity and is 10^6 times more RI α -specific. Thus, RIAD has clear advantages over existing reagents in delineating cAMP signaling events that depend on anchoring of type I PKA.

RIAD was derived from a high affinity RI α binding consensus sequence based on five linear R binding sequences from the dual affinity D-AKAP1 (11), AKAP149 (31), ezrin,⁴ and AKAP82 (two sequences, FSC1A and FSC1B) (13, 14). Consensus sequences derived from other combinations of RI α binding motifs were found to confer lower RI α affinity and were, therefore, not included. Further optimization of the consensus sequence by two-dimensional peptide arrays identified that acidic amino acids are important for high RI α specificity, and acidic amino acids were, therefore, substituted into specific positions in the sequence. The importance of acidic substitutions is consistent with the charged docking surface in N terminus of RI α (50) compared with the more hydrophobic docking surface of RII α . Structure determination of the RI α -RIAD complex will be important to reveal the differences in AKAP binding for type I versus type II PKA.

By adding arginine-rich sequences (Arg₁₁) to the peptides, RIAD-Arg₁₁ and scRIAD-Arg₁₁ (negative control) translocated rapidly and efficiently into the cells (~ 10 min),⁶ consistent with previous reports (51). The selectivity of RIAD for type I PKA was clearly demonstrated in two defined biological systems; RIAD had no effect on type II PKA-regulated AMPA-responsive currents in hippocampal neurons but clearly perturbed type I PKA-mediated inhibition of T cell function by displacing anchored type I PKA from lipid rafts, which reduced Tyr-505 phosphorylation of Lck and up-regulated T cell receptor signaling.

⁶ B. Lygren, K. Taskén, and C. R. Carlson, unpublished observations.

FIGURE 6. The effect of RIAD-Arg₁₁ on hormone-stimulated progesterone production in mouse Y1 adrenocortical cells. A, effect of anchoring disruption in the regulation of StAR phosphorylation and steroidogenesis. In the absence of hormonal stimuli, StAR levels are very low, and no cholesterol is transported into the mitochondria. Upon hormonal stimulation (left panel), cAMP activates anchored PKA type I, which is targeted to the mitochondria through binding to PAP7 (47). This results in phosphorylation of the newly synthesized StAR protein, up-regulation of the steroidogenic activity of StAR, and increased transport of cholesterol across the mitochondrial membrane through the peripheral benzodiazepine receptor (PBR). The side-chain cleavage cytochrome, P450_{ssc}, is the first enzyme in the steroidogenic pathway and is responsible for transformation of cholesterol into pregnenolone, which is further transformed into progesterone. RIAD disrupts the PKA-PAP7 interaction (right panel). As a result StAR is not phosphorylated upon hormonal stimulation. Thus, the steroidogenic activity of StAR as well as steroid biosynthesis is not up-regulated. The model was modified from (47). B, PKA-RI α (green) was displaced from mitochondria (visualized by MitoTracker Red) in Y1 adrenocortical cells treated with RIAD-Arg₁₁ (6 or 15 μM) for 12 h (upper panels). scRIAD-Arg₁₁ was used as a negative control (lower panels). C, schematic representation of a solid phase immobilization assay. Peptides synthesized in triplicate on membranes were incubated in Y1 adrenocortical cell lysate overnight, and immobilized proteins were eluted and analyzed by immunoblotting (WB, left panel). Levels of PKA-RI α and PKA-C immobilized by RIAD on solid phase after incubation in Y1 adrenocortical cell lysate are shown (right panel). D, levels of StAR in basal, forskolin-stimulated, or forskolin and actinomycin D (Act)-treated Y1 adrenocortical cells after treatment with 30 μM RIAD-Arg₁₁ or 30 μM scRIAD-Arg₁₁. E, forskolin-stimulated progesterone production in Y1 adrenocortical cells treated with RIAD-Arg₁₁ or scRIAD-Arg₁₁. Actinomycin D was used to block protein synthesis to avoid concomitant up-regulation of StAR levels (mean \pm S.E. from $n = 3$, $p < 0.01$).

Peptide hormones and cAMP are known to acutely stimulate steroid biosynthesis. However, steroidogenesis cannot be stimulated by corticotropin or cAMP analogues in a type I kinase-defective Y1 mouse adrenocortical cell line (52). In addition, PAP7 has been described to be involved in steroidogenesis by anchoring type I PKA together with the peripheral benzodiazepine receptor complex in mitochondria (17). It was, therefore, relevant to analyze the effect of RIAD on the putative type I PKA-PAP7-peripheral benzodiazepine receptor signaling pathway and steroidogenesis. Type I PKA was efficiently displaced from mitochondria in cells treated with RIAD, which led to inhibition of hormone-stimulated progesterone production. In comparison to mutating the PKA phosphorylation site in StAR (49), disruption of type I PKA anchoring by RIAD was ~80% effective in inhibiting steroid biosynthesis. This discrepancy is probably due to degradation of the peptide as the estimated half-life is 8–10 h in 10% serum.⁷ In conclusion, disruption of type I PKA anchoring by RIAD blocked the progesterone synthesis and confirmed that steroidogenesis is dependent on type I anchoring.

Collectively, our data show that RIAD is a potent disruptor of anchored PKA type I signaling *in situ*. By displacement of type I PKA by RIAD, cellular effects of PKA type I-dependent anchored signaling can be delineated in different cell types. Such experiments may reveal primary and secondary effects of type I-dependent signaling and identify novel downstream targets and relationships to other signaling pathways. Furthermore, signaling through PKA pathways plays an important role in many diseases, and RIAD may potentially also be used to elucidate whether disorders with a perturbed PKA signaling is dependent on anchored PKA type I.

Acknowledgments—We thank Gladys M. Tjørhom and Ola Blingsmo for technical assistance, Dimitris Mantzilas at the Institute of Molecular Biosciences at UiO for assistance with CD analysis, Neal Alto for introducing us to the use of peptide array synthesis, Torkel Vang for discussions regarding the cAMP-PKA-Csk-Lck signaling pathway, and Lorene Langeberg and members of the Scott and Taskén laboratories for helpful discussions.

REFERENCES

- Carnegie, G. K., Smith, F. D., McConnachie, G., Langeberg, L. K., and Scott, J. D. (2004) *Mol. Cell* **15**, 889–899
- Klauck, T. M., Faux, M. C., Labudde, K., Langeberg, L. K., Jaken, S., and Scott, J. D. (1996) *Science* **271**, 1589–1592
- Tasken, K., and Aandahl, E. M. (2004) *Physiol. Rev.* **84**, 137–167
- Alto, N., Michel, J. J. C., Dodge, K. L., Langeberg, L. K., and Scott, J. D. (2002) *Diabetes* **51**, 385–388
- Coghlan, V. M., Perrino, B. A., Howard, M., Langeberg, L. K., Hicks, J. B., Gallatin, W. M., and Scott, J. D. (1995) *Science* **267**, 108–111
- Baillie, G. S., Scott, J. D., and Houslay, M. D. (2005) *FEBS Lett.* **579**, 3264–3270
- Dodge-Kafka, K. L., Soughayer, J., Pare, G. C., Michel, J. J. C., Langeberg, L. K., Kapiloff, M. S., and Scott, J. D. (2005) *Nature* **437**, 574–578
- Dodge, K. L., Khouangsathiene, S., Kapiloff, M. S., Mouton, R., Hill, E. V., Houslay, M. D., Langeberg, L. K., and Scott, J. D. (2001) *EMBO J.* **20**, 1921–1930
- Tasken, K. A., Collas, P., Kemmners, W. A., Witczak, O., Conti, M., and Tasken, K. (2001) *J. Biol. Chem.* **276**, 21999–22002

⁷ E. Torheim, K. Taskén, and C. Carlson, unpublished observations.

- Wong, W., and Scott, J. D. (2004) *Nat. Rev. Mol. Cell Biol.* **5**, 959–970
- Huang, L. J. S., Durick, K., Weiner, J. A., Chun, J., and Taylor, S. S. (1997) *J. Biol. Chem.* **272**, 8057–8064
- Wang, L., Sunahara, R. K., Kruminis, A., Perkins, G., Crochiere, M. L., Mackey, M., Bell, S., Ellisman, M. H., and Taylor, S. S. (2001) *Proc. Natl. Acad. Sci. U. S. A.* **98**, 3220–3225
- Carrera, A., Gerton, G. L., and Moss, S. B. (1994) *Dev. Biol.* **165**, 272–284
- Miki, E., and Eddy, E. M. (1998) *J. Biol. Chem.* **273**, 34384–34390
- Li, H. W., Adamik, R., Pacheco-Rodriguez, G., Moss, J., and Vaughan, M. (2003) *Proc. Natl. Acad. Sci. U. S. A.* **100**, 1627–1632
- Angelo, R., and Rubin, C. S. (1998) *J. Biol. Chem.* **273**, 14633–14643
- Li, H., Degenhardt, B., Tobin, D., Yao, Z. X., Tasken, K., and Papadopoulos, V. (2001) *Mol. Endocrinol.* **15**, 2211–2228
- Gronholm, M., Vossebein, L., Carlson, C. R., Kuja-Panula, J., Teesalu, T., Alftan, K., Vaheri, A., Rauvala, H., Herberg, F. W., Tasken, K., and Carpen, O. (2003) *J. Biol. Chem.* **278**, 41167–41172
- Carr, D. W., Hausken, Z. E., Fraser, I. D. C., Stofkohahn, R. E., and Scott, J. D. (1992) *J. Biol. Chem.* **267**, 13376–13382
- Diviani, D., Soderling, J., and Scott, J. D. (2001) *J. Biol. Chem.* **276**, 44247–44257
- Burns-Hamuro, L. L., Ma, Y. L., Kammerer, S., Reineke, U., Self, C., Cook, C., Olson, G. L., Cantor, C. R., Braun, A., and Taylor, S. S. (2003) *Proc. Natl. Acad. Sci. U. S. A.* **100**, 4072–4077
- Frank, R. (1992) *Tetrahedron* **48**, 9217–9232
- Bailey, T. L., and Elkan, C. (1994) *Proc. Int. Conf. Intell. Syst. Mol. Biol.* **2**, 28–36
- Hausken, Z. E., Coghlan, V. M., and Scott, J. D. (1998) *Methods Mol. Biol.* **88**, 47–64
- Aandahl, E. M., Aukrust, P., Skalhogg, B. S., Muller, F., Froland, S. S., Hansson, V., and Tasken, K. (1998) *FASEB J.* **12**, 855–862
- Corbin, J. D., and Reimann, E. M. (1974) *Methods Enzymol.* **38**, 287–290
- Scott, J. D., Glaccum, M. B., Fischer, E. H., and Krebs, E. G. (1986) *Proc. Natl. Acad. Sci. U. S. A.* **83**, 1613–1616
- Herberg, F. W., Maleszka, A., Eide, T., Vossebein, L., and Tasken, K. (2000) *J. Mol. Biol.* **298**, 329–339
- Birkemo, G. A., Mantzilas, D., Luders, T., Nes, I. F., and Nissen-Meyer, J. (2004) *Biochim. Biophys. Acta* **1699**, 221–227
- Lygren, B., Tasken, K., and Carlson, C. R. (2005) *J. Immunol. Methods* **305**, 199–205
- Trendelenburg, G., Hummel, M., Riecken, E. O., and Hanski, C. (1996) *Biochem. Biophys. Res. Commun.* **225**, 313–319
- Durgerian, S., and Taylor, S. S. (1989) *J. Biol. Chem.* **264**, 9807–9813
- Rosenmund, C., Carr, D. W., Bergeson, S. E., Nilaver, G., Scott, J. D., and Westbrook, G. L. (1994) *Nature* **368**, 853–856
- Aandahl, E. M., Moretto, W. J., Haslett, P. A., Vang, T., Bryn, T., Tasken, K., and Nixon, D. F. (2002) *J. Immunol.* **169**, 802–808
- Skalhogg, B. S., Landmark, B. F., Doskeland, S. O., Hansson, V., Lea, T., and Jahnsen, T. (1992) *J. Biol. Chem.* **267**, 15707–15714
- Skalhogg, B. S., Tasken, K., Hansson, V., Huitfeldt, H. S., Jahnsen, T., and Lea, T. (1994) *Science* **263**, 84–87
- Abrahamsen, H., Vang, T., and Tasken, K. (2003) *J. Biol. Chem.* **278**, 17170–17177
- Torgersen, K. M., Vang, T., Abrahamsen, H., Yaqub, S., Horejsi, V., Schraven, B., Rolstad, B., Mustelin, T., and Tasken, K. (2001) *J. Biol. Chem.* **276**, 29313–29318
- Vang, T., Torgersen, K. M., Sundvold, V., Saxena, M., Levy, F. O., Skalhogg, B. S., Hansson, V., Mustelin, T., and Tasken, K. (2001) *J. Exp. Med.* **193**, 497–507
- Vang, T., Abrahamsen, H., Myklebust, S., Horejsi, V., and Tasken, K. (2003) *J. Biol. Chem.* **278**, 17597–17600
- Mustelin, T., and Tasken, K. (2003) *Biochem. J.* **371**, 15–27
- Witczak, O., Skalhogg, B. S., Keryer, G., Bornens, M., Tasken, K., Jahnsen, T., and Orstavik, S. (1999) *EMBO J.* **18**, 1858–1868
- Weber, J. R., Orstavik, S., Torgersen, K. M., Danbolt, N. C., Berg, S. F., Ryan, J. C., Tasken, K., Imboden, J. B., and Vaage, J. T. (1998) *J. Exp. Med.* **187**, 1157–1161
- Zhang, W. G., Sloan-Lancaster, J., Kitchen, J., Tribble, R. P., and Samelson, L. E. (1998) *Cell* **92**, 83–92

45. Sewer, M. B., and Waterman, M. R. (2001) *Rev. Endocr. Metab. Disord.* **2**, 269–274
46. Stocco, D. M. (2001) *Annu. Rev. Physiol.* **63**, 193–213
47. Liu, J., Li, H., and Papadopoulos, V. (2003) *J. Steroid Biochem. Mol. Biol.* **85**, 275–283
48. Jo, Y., King, S. R., Khan, S. A., and Stocco, D. M. (2005) *Biol. Reprod.* **73**, 244–255
49. Arakane, F., King, S. R., Du, Y., Kallen, C. B., Walsh, L. P., Watari, H., Stocco, D. M., and Strauss, J. F. (1997) *J. Biol. Chem.* **272**, 32656–32662
50. Banky, P., Newlon, M. G., Roy, M., Garrod, S., Taylor, S. S., and Jennings, P. A. (2000) *J. Biol. Chem.* **275**, 35146–35152
51. Futaki, S. (2005) *Adv. Drug Delivery Rev.* **57**, 547–558
52. Clegg, C. H., Abrahamsen, M. S., Degen, J. L., Morris, D. R., and Mcknight, G. S. (1992) *Biochem.* **31**, 3720–3726